Automated pole selection using the DERRP methodology

N. Pandiya [1,2], **W. Desmet** [2,3]
[1] Robert Bosch GmbH, Center of Competence-Vibration,
71701 Schwieberdingen, Germany
e-mail: **nimish.pandiya@de.bosch.com**

[2] KU Leuven, Department of Mechanical Engineering,
Celestijnenlaan 300, B-3001, Heverlee, Belgium

[3] DMMS Core Lab, Flanders Make, Belgium

Abstract
A new parameter estimation procedure called Direct Estimation of Residuals from Rational-fraction Polynomials (or DERRP) was recently introduced, wherein estimation of all modal parameters is done in a single global computational step. Hence, reconstruction of FRFs is made possible at the traditional pole-selection step in a modified stabilisation chart. The novelties in the stabilisation chart include additional comparisons of residues, residuals and the "longest vector". An automated model order determination strategy based on the error between the DERRP-reconstructed and the experimental FRFs is presented in the paper. The work aims to minimize the reliability on user-expertise and a provide a mathematical basis for the construction of a valid structural modal model. The applicability of the aforementioned methods is demonstrated using a FRF dataset obtained for an e-bike frame, the underlying aim for which was to provide an insight to its dynamic behavior and determination of loads at component level.

1 Introduction

Modal parameter estimation (MPE) refers to a system identification procedure for vibrating mechanical structures where an *a-priori* model is used to determine structural modal parameters from Frequency Response Functions (FRFs) or Impulse Response Functions (IRFs). It is a well-researched topic with various approaches proposed over the past decades, and its maturity may be gauged by the availability of a common framework unifying the various algorithms - UMPA (Unified Matrix Polynomial Approach) [1] and the widespread use of algorithms like the poly-reference least squares frequency domain approach (also called PolyMAX© [2]) for industrial use cases. One of long-lasting focuses of research in the field is the automation of the MPE process [3, 4, 5] such that it may be used as a "commodity-tool" [6] by less experienced engineers and/or technicians [7]. The estimation of a modal model from experimental data, however, relies heavily on user expertise and experience, especially for selecting valid structural poles from stabilisation charts. Herein lies the motivation for the presented work: to provide a mathematical foundation for the same and augment it with statistical principles to automate the MPE process. The goal is that FRF data should be fed to the algorithm and an accurate modal model must be estimated without user interaction. The ideology behind the algorithm is to compare the modal model based on the ultimate validation strategy - comparison of synthesized FRFs with the measured ones.

2 Theoretical background

The modal parameters that characterise the dynamics of a Multiple-Input Multiple-Output (MIMO), Linear Time Invariant (LTI) system are as follows:

- **Poles or complex natural frequencies** ($\lambda = \sigma + j\Omega$): The imaginary part corresponds to the observable damped natural frequency while the real part is called the damping factor.
- **Modal (or mode shape) vectors** ($\{\psi\}$) represent the principal shapes that the structure assumes when vibrating at its natural frequency.
- **Participation vectors** ($\{L\}$) represent the contribution of various force input degrees-of-freedom (DoFs) to each of the mode shapes.
- **Modal scaling factors** (Q) represents the constant that scales a normalised mode shape.

MPE starts with FRF data acquisition, where responses and (force) references are measured at different Degrees of Freedom (DoFs). These are used to compute FRFs (or IRFs) that are further used to estimate the modal parameters. The FRF matrix ($[H(\omega)] \in \mathbb{C}^{N_o \times N_i}$) relating displacements to forces is represented in the partial fraction description of the MIMO FRF matrix in the frequency (or Fourier) domain in terms of the residues ($[A_r] \in \mathbb{C}^{N_o \times N_i}$), poles ($\lambda_r$) and residuals, both lower ($[LR] \in \mathbb{C}^{N_o \times N_i}$) and upper($[UR] \in \mathbb{C}^{N_o \times N_i}$), as shown in Equation (1).

$$\Big[H(\omega)\Big]_{N_o \times N_i} = \sum_{r=1}^{N_r} \left(\frac{[A_r]_{N_o \times N_i}}{j\omega - \lambda_r} + \frac{[A_r]^*_{N_o \times N_i}}{j\omega - \lambda_r^*} \right) + \frac{[LR]_{N_o \times N_i}}{(j\omega)^2} + [UR]_{N_o \times N_i} \tag{1}$$

Here, N_o is the number of outputs, N_i is the number of inputs and N_r is the number of conjugate mode pairs ($\lambda_r, \lambda_r^* = \sigma \pm j\Omega$).

The residue at the r^{th} non-repeated modal frequency (*i.e.* $[A_r]$) is of unity rank and can be decomposed into the modal scaling factor ($Q_r \in \mathbb{C}^{1\times1}$), the modal vector ($\psi_r \in \mathbb{C}^{N_o\times1}$) and the modal participation vector ($L_r \in \mathbb{C}^{N_i\times1}$) as shown in Equation (2). For the proportionally damped case, the residue is purely imaginary.

$$\big[A_r\big]_{N_o \times N_i} = Q_r \big\{\psi_r\big\}_{N_o \times 1} \big\{L_r\big\}^T_{1 \times N_i} \tag{2}$$

A rational fraction polynomial (RFP) is often used to represent the FRF matrix to initiate the MPE process. The left-matrix RFP description shown in Equation (3), is used to construct an overdetermined set of equations at each frequency line ($s = j\omega$), which is then solved in a least squares sense for the shown matrix polynomial coefficients of the "denominator"($[\alpha_i]$) and the "numerator" ($[\beta_i]$).

$$\Big[H(s)\Big]_{N_o \times N_i} = \left[\sum_{i=0}^{m} \Big[[\alpha_i]s^i\Big]\right]^{-1}_{N_o \times N_o} \left[\sum_{i=0}^{m} \Big[[\beta_i]s^i\Big]\right]_{N_o \times N_i} \tag{3}$$

The "numerator" (or $[\beta_i]$) matrix coefficients are then either ignored after, or eliminated by substitution (using normal equations) before, the least squares solution. This is the first stage of the traditional two-step approach where only the "denominator" (or $[\alpha_i]$) matrix coefficients are kept, and are used to develop a polynomial eigen-value solution [8] (also see companion matrix [9]). This process is carried out for increasing model order m, resulting in complex poles (as eigen-values) and modal vectors (as truncated eigen-vectors) for each model order iteration, using which a consistency (or stabilisation) chart may be plotted.

The user is then required to select valid poles from the large set of computed poles (and associated modal vectors). This is an important step in the first stage of MPE and requires user experience, especially when the data set may be noisy. Only after the poles are expertly selected and finalised, may the user proceed to the second stage where the partial fraction model is applied (Equation (1)) to each frequency line to compute the participation vectors, modal scaling, and the upper and lower residuals in a least squares sense.

2.1 Global MPE using DERRP

The recently introduced Direct Estimation of Residuals from Rational-fraction Polynomials (or DERRP) algorithm [10, 11] estimates all the parameters in a single computation step, before the construction of

the stabilisation chart. Hence, the complete set of modal parameters is available and each model-order's synthesized FRFs can theoretically be validated against the original experimental set.

Under the DERRP methodology, the partial fraction model shown in Equation (1) is explicitly expanded to a RFP, using a left-matrix description (LMD) (Equation (4)). The "numerator" matrix polynomial order is limited to one lesser than that of the "denominator" matrix polynomial to ensure stability of the system.

$$\Big[H(s)\Big]_{N_o \times N_i} = \left[\sum_{i=0}^{m}\Big[[\alpha_i]s^i\Big]\right]^{-1}_{N_o \times N_o}\left[\sum_{i=0}^{m-1}\Big[[\beta_i]s^i\Big]\right]_{N_o \times N_i} + \frac{[LR]_{N_o \times N_i}}{s^2} + [UR]_{N_o \times N_i} \tag{4}$$

Through left multiplication, this equation is simplified to Equation (5) to include the residual terms in a modified RFP-LMD.

$$\left[\sum_{i=0}^{m}\Big[[\alpha_i][H(s)]s^i\Big]\right] - \left[\sum_{i=-2}^{m}\Big[[\hat{\beta}_i][I]s^i\Big]\right] = \Big[0\Big] \tag{5}$$

As for Equation (3), an overdetermined least-squares setup using Equation (5) computes the matrix-coefficients $[\alpha_i]$ and $[\hat{\beta}_i]$ for increasing model iteration m. The "numerator" is then explicitly expressed as a ratio of the adjoint matrix-coefficient polynomial and the characteristic polynomial (Equation (6)) using Vu's extension of Faddeev's algorithms [12].

$$\left[\sum_{i=0}^{m}\Big[[\alpha_i]s^i\Big]\right]^{-1}_{N_o \times N_o} = \frac{\left[\sum_{i=0}^{(N_o-1)m}\Big[[\alpha_i^+]s^i\Big]_{N_o \times N_o}\right]}{\sum_{i=0}^{N_o m} d_i s^i} \tag{6}$$

This allows the MIMO model to be represented in its common-denominator form as shown in Equation (7).

$$\sum_{r=1}^{N_r}\left(\frac{[A_r]_{N_o \times N_i}}{s-\lambda_r} + \frac{[A_r]^*_{N_o \times N_i}}{s-\lambda_r^*}\right) + \frac{[LR]_{N_o \times N_i}}{s^2} + [UR]_{N_o \times N_i} = \frac{\left[\sum_{i=0}^{(N_o-1)m}\Big[[\alpha_i^+]s^i\Big]_{N_o \times N_o}\right]\left[\sum_{i=-2}^{m}\Big[[\hat{\beta}_i]s^i\Big]_{N_o \times N_i}\right]}{\sum_{i=0}^{N_o m} d_i s^i} \tag{7}$$

By a simple comparison of the LHS (theoretical model) and RHS (available model) in Equation (7), the (r^{th}) modal parameters are calculated as follows.

- **Poles or complex natural frequencies** ($\lambda_r = \sigma_r + j\Omega_r$) are the roots of the monic characteristic equation (denominator of the RHS in Equation (7)).
- **Modal Residue**($[A_r]$) associated with the pole λ_r is computed using Equation (8) using L'Hospitals rule for ratio of indeterminate forms.

$$\Big[A_r\Big]_{N_o \times N_i} = \lim_{s \to \lambda_r}\Big(\Big[H(s)\Big] * (s-\lambda_r)\Big) \tag{8}$$

  Equation (9) shows the derived final expression for the residue, which is of unity rank due to the absence of truly repeated roots in actual dynamic systems. A singular value decomposition explicitly results in the mode shape, participation vector and modal scaling for each pole.

$$\Big[A_r\Big]_{N_o \times N_i} = \left.\frac{\left[\sum_{i=0}^{(N_o-1)m}\Big[[\alpha_i^+]s^i\Big]\right]\left[\sum_{i=-2}^{m}\Big[[\hat{\beta}_i]s^i\Big]\right]}{\sum_{i=1}^{N_o m} i d_i s^{i-1}}\right|_{s=\lambda_r} \tag{9}$$

- **Lower and Upper Residuals** are calculable as the residue at $s \to 0$ and at $s \to \infty$ respectively.
- **Longest vector**($\hat{\psi}_r$) is a recently developed [13, 14] derived parameter that combines information from both the modal and participation vectors to identify the modal deflections for all uniquely measured DoFs. Apart from an additional filtering criteria in the stabilisation chart, the longest vector can also be used to predict unmeasured (driving point) FRFs and visualisation of a "virtual" mode shape, such that all measured (input or output) DoFs are animated.
  The condensed description of the information included in the modal and participation vectors ($\{\psi\}$ and ($\{L\}$ respectively) is done by rotating and scaling either of the two such that the common components (from driving point DoFs) are coincident or have the smallest distance in a least-squares sense. The vector with the higher mean phase correlation (MPC) is chosen to be rotated by an angle that is the difference of their mean phases.

Thus, all parameters that define the admittance transfer function (Equation (1)) in a finite frequency range of interest are obtained before the traditional stabilisation chart is plotted. The stabilisation chart is hence modified such that in addition to an iteration-wise comparison of the modal vector, the participation vector (in other words, the complete scaled modal residue), the "longest" vector and the residuals are also included in this comparison [11].

As the model order m increases, so do the number of computed poles and associated modal parameters. This increase reflects the overfitting of available FRF data and manifests in the increase in the number of inconsistent computational poles, while the same structural poles are ideally computed for each model order[15]. Consequently, the computational poles are required to be sorted out for the user to choose valid poles only from an effective set of structural poles. The real and imaginary parts of a pole (representing damping factor and damped natural frequency) are typically checked to be within a tolerance percentage to another pole that represents the same resonance condition. The percentage of similarity for the modal, participation and longest vectors, on the other hand, is computed by using Modal Assurance Criterion (MAC) [16](Equation (10)).

$$MAC_{v_1,v_2} = \frac{|\{v_1\}^H\{v_2\}|^2}{\{v_1\}^H\{v_1\}\{v_2\}^H\{v_2\}} * 100\% \tag{10}$$

The lower and upper residuals are computed explicitly and are separately compared iteration wise. This comparison is done by reshaping the entire residual matrix as a vector and using the synthesis correlation coefficient definition [9] to represent the percentage similarity. It should be noted that in presence of noise, this estimate is not the best, but only one possibility. If multiple bands are merged, the residuals naturally need to be computed again.

$$diff = \frac{|\sum(R_{1i}R_{2i}^*)|^2}{\{\sum(R_{1i}R_{1i}^*)\}\{\sum(\sum(R_{1i}R_{2i}^*\}} * 100 \tag{11}$$

2.2 Existing automatic pole selection techniques

The aforementioned selection of valid structural poles is the biggest hurdle in automation of the MPE process. A high level of expertise is required, and even then, the results may vary depending on the individual judgements of users. Plenty of effort has been put into clearing up the stabilisation charts of computational poles and create fast stabilising charts. The focus, however, remains largely on the visual aspect of the chart, and that the user must find the pole-selection process easy and time-efficient. A good overview of existing techniques and proposals that are more generally applicable is provided in [17, 5]. The idea behind most techniques relies heavily on MAC comparisons of mode shapes and analysing clusters of poles computed from increasing model order iterations [7]. Other methods include fuzzy clustering techniques [18] and histogram separation [19]. However, for automated algorithms, there exist threshold values (like number of stable poles required, or realistic damping factor values for poles that "pollute" the set of structural poles etc.) that should be input by the user, and this in turn requires even more user expertise.

However, the automation strategies in literature are based on usage of incomplete modal models *i.e.*, only the vector and pole information are available. With an increase in the present-day computing power, using DERRP, a complete modal model for each model-order iteration can be computed. This allows an error-based, automatic selection of poles such that no user interaction is required between feeding the algorithm with data and assessing the results.

It is worthwhile to mention the various stages apart from the data input and assessment where the user must interact with the algorithm:

- The user typically needs to input at least the maximum model order based on how many peaks are generally seen within the frequency range of interest. This is known as model order determination.
- Selection of poles is the main task requiring user expertise.

The strategy that is generally followed in this work is:

- The stabilisation chart is cleared of **all** spurious poles by employing criteria that indicate or refute their structural nature.
- Model order determination is carried out based on the maximum equations that can be formed for the least squares step. Additionally, a new metric is proposed which allows model orders to be determined based on the accuracy of the resulting curve fit.

3 Proposed automated MPE methodology

3.1 Model order determination

The key advantage of DERRP is that the residuals are also computed per iteration. Hence it is useful if the structural poles are all selected from the same iteration. In fact, rather than structural pole selection, the problem statement can be transformed to pick the correct model order iteration.

Since the complete modal model (including out-of-band residual effects) is available, a numerical comparison of the similarity between the obtained model against the FRF measurements can be made. The FRF Similarity Metric was introduced in [20] which computes the similarity in the powers of two FRFs based on a maximum likelihood estimator. The FRF matrix is synthesized $\hat{H}$ (Equation (1)) and compared to the measured one for each iteration.

$$FRFSM_{H_{pq},\hat{H}_{pq}} = \frac{1}{N_f}\sum_{j=1}^{N_f}\frac{f(\epsilon_j(H_{pq},\hat{H}_{pq});0,\sigma_0^2)}{f(0;0,\sigma_0^2)} \tag{12}$$

The probability density function f is assumed to be Gaussian as shown in Equation (13).

$$f(x;\mu,\sigma^2) = \frac{1}{\sigma\sqrt{2\pi}}e^{-\frac{1}{2}(\frac{x-\mu}{\sigma})^2} \tag{13}$$

The error $\epsilon_j(H_{pq},\hat{H}_{pq})$ for the j^{th} frequency, is the difference of magnitudes, defined in the decibel scale as shown in Equation (14).

$$\epsilon_j(H_{pq},\hat{H}_{pq}) = |10\log_{10}(H_{pq}(s_j)) - 10\log_{10}(\hat{H}_{pq}(s_j))| \tag{14}$$

According to [20], the value of σ_0 is taken as 6, corresponding to the half power of the automoment curve. To this effect, a new metric called the Automoment-FRFSM (AMFRFSM) is proposed, that compares the automoment (Equation (16)) of the measured and the synthesised FRF matrix (M and $\hat{M}$ respectively).

$$AMFRFSM_{M,\hat{M}} = \frac{1}{N_f}\sum_{j=1}^{N_f}\frac{f(\epsilon_j(M,\hat{M});0,\sigma_0^2)}{f(0;0,\sigma_0^2)} \tag{15}$$

where, ϵ_j is defined in Equation (14) and the automoment is defined as in Equation (16).

$$M(s) = \sqrt{\frac{1}{N_o N_i}|H(s)|^2} \tag{16}$$

3.2 Pole in FRF Automoment Confidence for pole sorting

For each pole estimated, a new criterion called the Pole in FRF Automoment Confidence (or PiFAC) is hereby proposed. The effect of the concerned pole is deducted from the measured FRF to indicate the effect of the r^{th} pole's residue on the system (Equation (17)).

$$H_r(s) = H - \left(\frac{[A_r]_{N_o \times N_i}}{j\omega - \lambda_r} + \frac{[A_r]^*_{N_o \times N_i}}{j\omega - \lambda^*_r} \right) \tag{17}$$

To globalise the effects of the poles, the automoment for the resulting matrix (M_r) is computed from H_r according to Equation (16) to be compared against the same for the measured FRFs, using the AMFRFSM metric introduced in Equation (18).

$$FRFSM_{M,\hat{M}} = \frac{1}{N_f} \sum_{j=1}^{N_f} \frac{f(\epsilon_j(M, M_r); 0, \sigma_0^2)}{f(0; 0, \sigma_0^2)} \tag{18}$$

PiFAC for the r^{th} mode in each model order, is then defined as:

$$PiFAC_r = 1 - FRFSM_{M,\hat{M}} \tag{19}$$

It must be noted that the FRFSM value does not incorporate frequency shifts or phase errors. For the current scenario however, these are unnecessary since the aim is to identify the absolute contribution of a pole in automoment curve. Based on low values of the PiFAC, poles are accepted as structural poles, or rejected as spurious poles. However, for FRF comparisons, it might be useful to consider the error and weights as shown in [21].

4 Application example

An E-bike frame was tested under free-free condition using the roving impact strategy to gather information about its modal behaviour. Figure 1 shows the free-free setup and the wireframe model used. A total of 130 impact locations were identified and acceleration was measured at a single point using a triaxial accelerometer as reference ($N_o = 3$). It must be noted that no impact was possible along the local Y-direction of the response location, while impacts were possible in the local X and Z directions ($N_i = 131$).

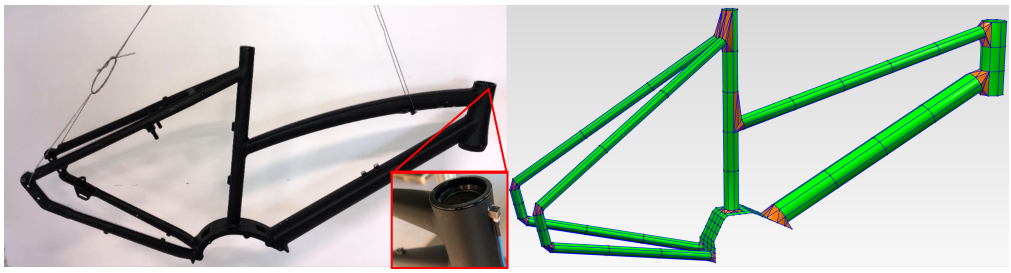

Figure 1: Free-free setup for the E-bike frame (left) and the wireframe model (right).

Figures 2 and 3 show the LTI nature of the system via reciprocity and driving point FRF plots respectively.

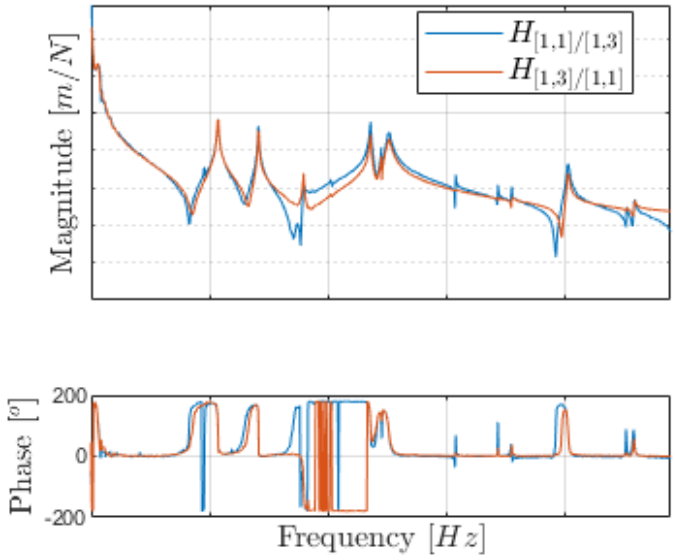

Figure 2: Reciprocity check between DoFs [1, 1] and [1, 3], i.e. point number 1 (reference accelerometer) in the local X and Z directions.

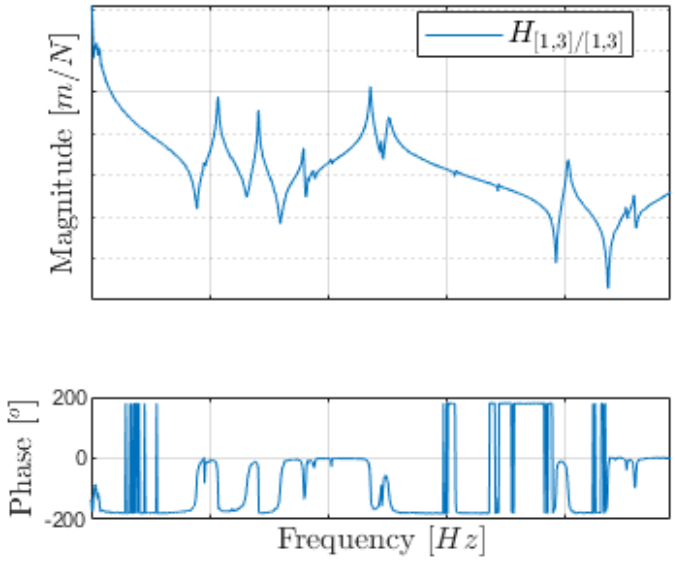

Figure 3: Driving point FRF check for DoF [1, 3], i.e. point number 1 local Z direction.

The complete frequency axis was selected to carry out the DERRP MPE process based on the frequency range of interest, and the good quality of data obtained.

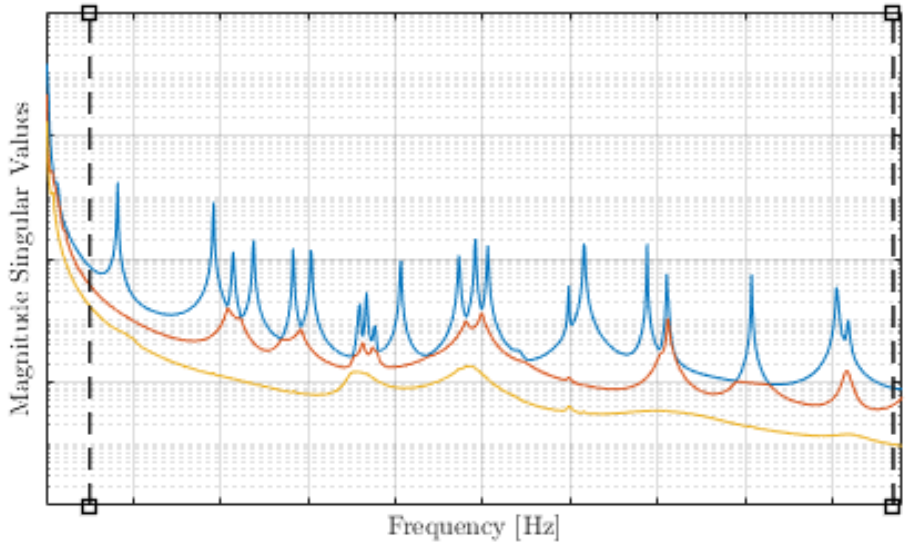

Figure 4: Complex Mode Indicator Function showing 20 clear peaks.

MPE using DERRP was then carried out and the stabilisation chart plotted, as shown in Figure 5. A clear stabilisation diagram is plotted with DERRP such that the poles are easily identifiable. However, as highlighted in Figure 5, there exist a trail of possibly overfitted poles (or possibly poorly excited modes) in the stabilisation chart. From a manual pole-selection point of view, it is difficult to select any pole from the first highlighted trail, and choose the correct model order from the second highlighted trail.

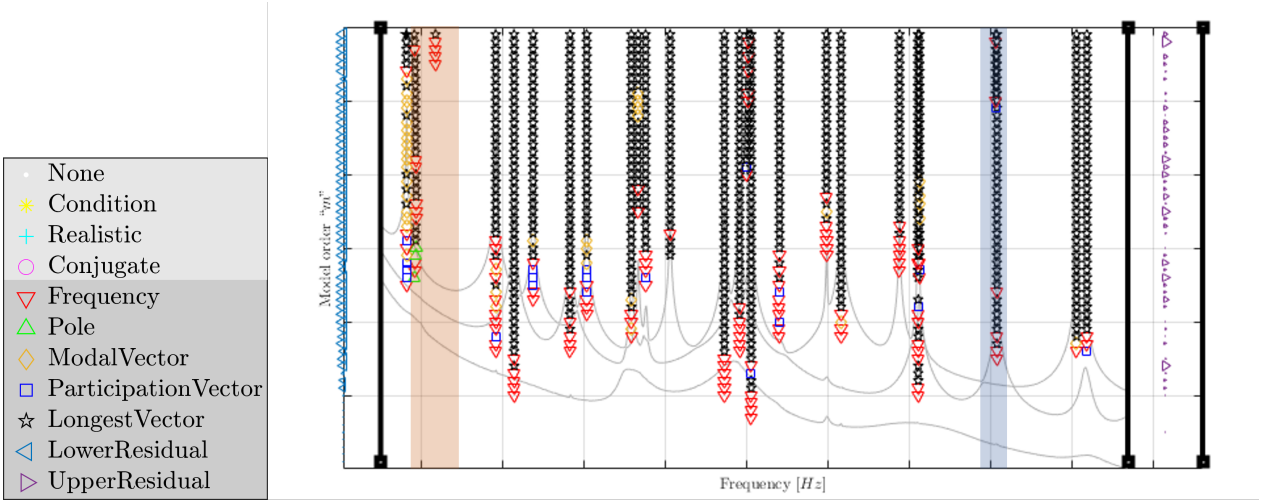

Figure 5: DERRP modified stabilisation chart.

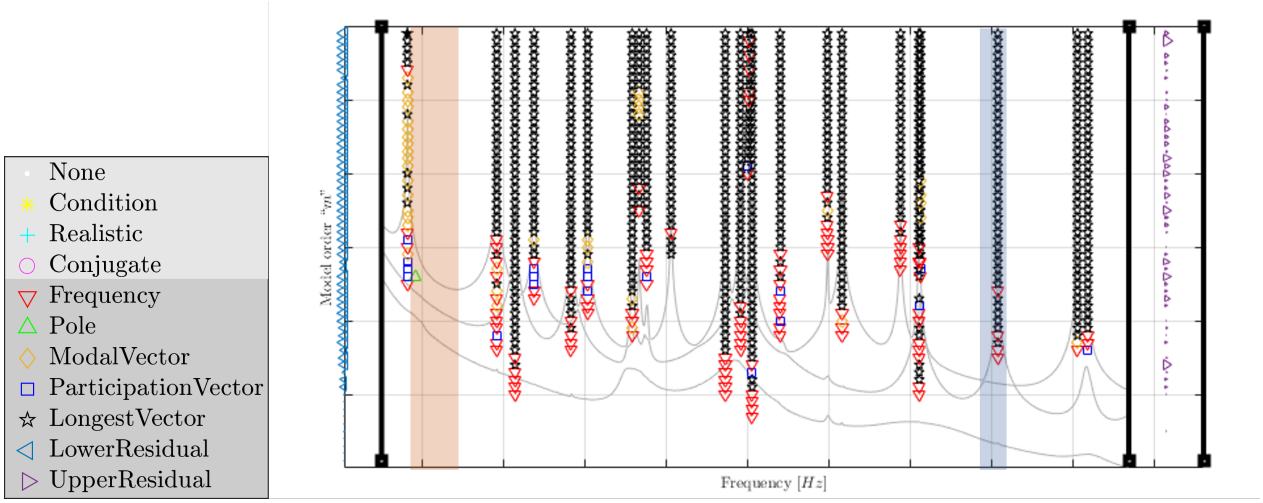

Figure 6: DERRP modified stabilisation chart with an additional filter of PiFAC value grater that 0.05.

The stabilisation chart is then plotted again with a new PiFAC > 0.05 criteria (more than a negligible zero value), and it is seen that the highlighted (orange) pole trails clear out from what are poorly estimated structural (in other words, spurious) poles for the given model order. It is also, seen that at higher model orders, the pole trail splits (blue). Using the PiFAC value, these over-fitted poles are also eliminated. The advantage of clearing out the stabilisation chart is that the synthesised automoment curve may be compared to the measured curve, to numerically select the iteration with the highest AMFRFSM value. This would then be the model order iteration containing most or all of the structural poles (Figure 7). Additionally, this strategy can also be used to carry out model order determination - when the AMFRFSM value plateaus (iteration 31, for e.g. in Figures 7 and 8), further model iterations need not be computed.

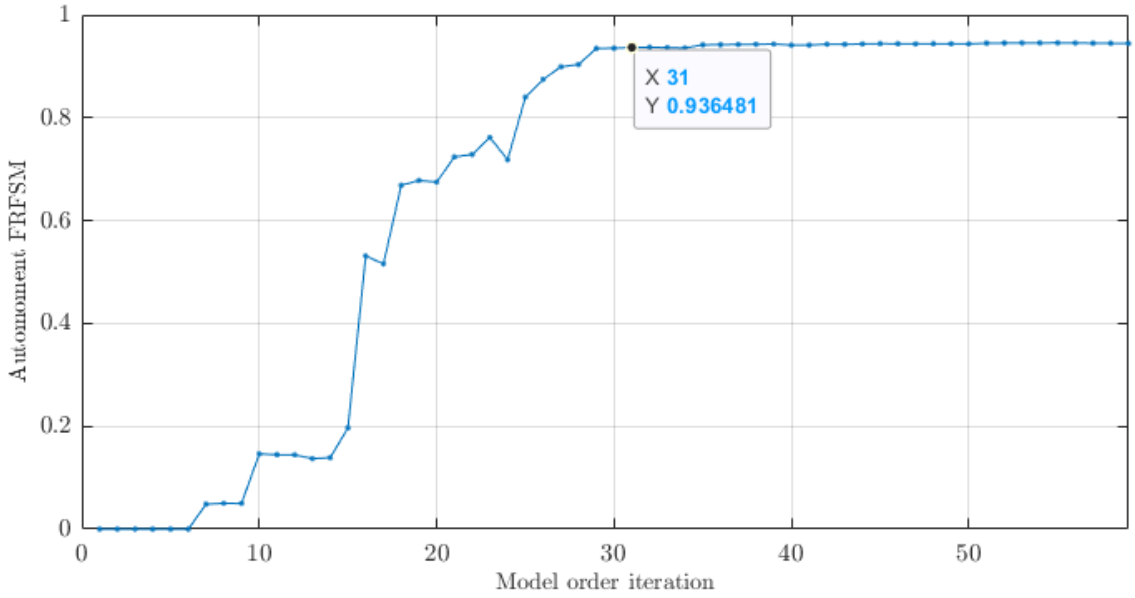

Figure 7: AMFRFSM values based on comparison of the automoment curves.

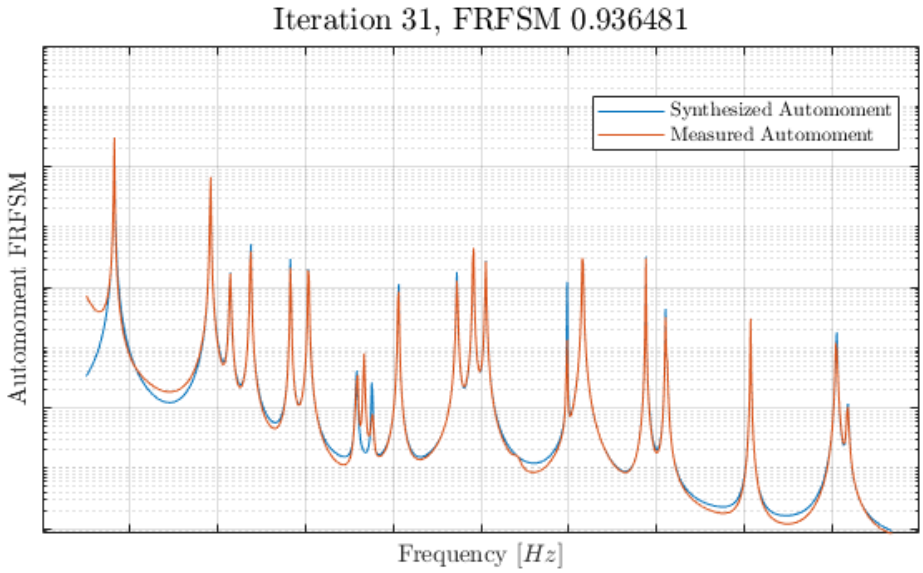

Figure 8: Comparison of the automoment curves for model order iteration 31.

Additionally, poles may be interactively chosen (by an expert user) through the AMFRFSM comparison using the selected ones. This provides the user a numerical basis for selection of poles (and associated modal parameters) from the same pole trail, but from a different iteration. This is shown in Figure 9, where the AMFRFSM value is slightly improved.

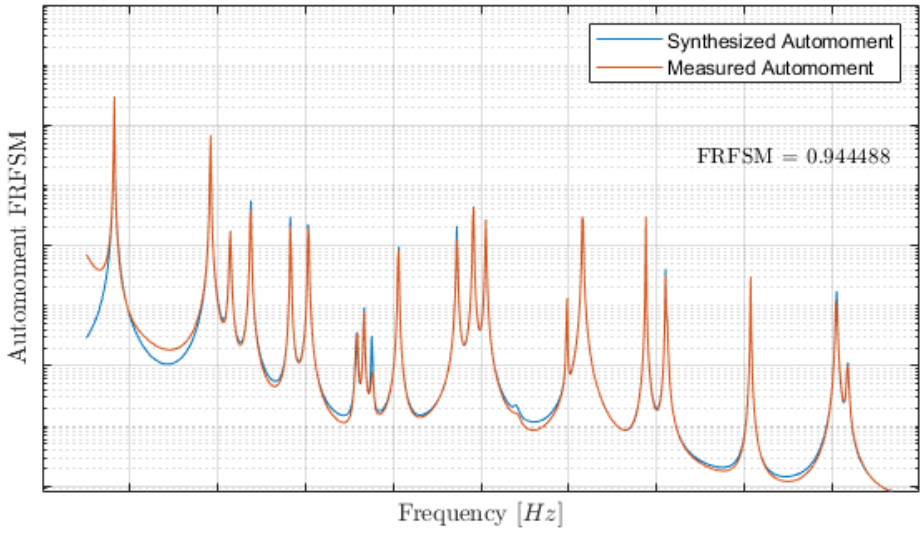

Figure 9: AMFRFSM values based on comparison of the automoment curves for a manual selection of poles and residuals.

In both the above stabilisation charts, the difference between the participation vector (long dimension i.e. 131 DoFs) and the longest vector [14] (unique measurement DoFs i.e. 132) must be noted. Even though the impact at the response node 1 was not possible in the local Y direction, its modal deflection is also predicted. An example is shown in Figure 10.

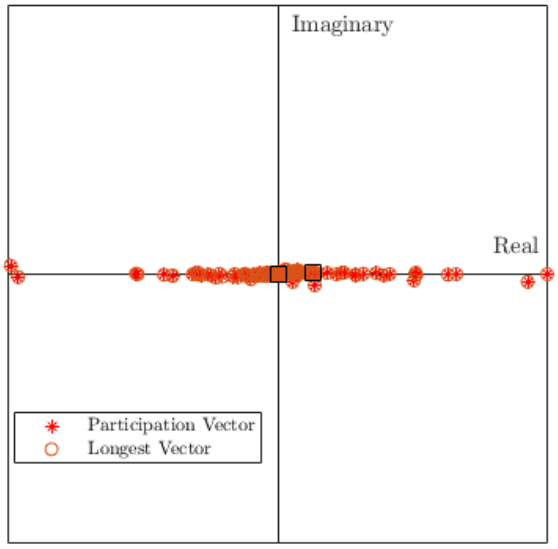

Figure 10: Longest vector(133×1) compared to the long dimension participation vector (131×1). The predicted modal deflection values are highlighted using the black squares.

5 Conclusion

The paper introduced a strategy for automatic pole selection based on the recently introduced MPE method called DERRP. The advantage of DERRP is that it predicts all modal parameters in a single computation stage, and these are made available during the pole selection phase. As such, instead of selecting poles based on a limited set of modal parameters, an error-based method is introduced which selects the modal parameters based on the best fit to the measured data. It is shown that the poles are first filtered out using traditional stabilisation chart filters (consistency in frequency, damping and mode shape), DERRP specific filters (participation and longest vector), and a novel confidence value named PiFAC or Pole in FRF Automoment Confidence value ranging from 0 to 1. The strategy is applied to a roving impact hammer FRF dataset obtained from an e-bike frame. It should be noted that the PiFAC value may be also defined as in [21] for the Maximum Likelihood Estimator, the variance being calculated based on the coherences. This is deemed as future work in addition to statistically determining the modal parameters from the set of poles having the highest PiFAC values.

Acknowledgements

The authors gratefully acknowledge the European Commission for its support of the Marie Sklodowska Curie program through the ETN PBNv2 project (GA 721615), and Mr. Jakob Duerr and Dr. Hubertus Ring from Bosch E-Bike Systems for acquired data.

References

[1] R. J. Allemang and D. Brown, “A unified matrix polynomial approach to modal identification,” *Journal of Sound and Vibration*, vol. 211, no. 3, pp. 301–322, 1998.

[2] P. Guillaume, P. Verboven, S. Vanlanduit, H. Van Der Auweraer, and B. Peeters, "A poly-reference implementation of the least-squares complex frequency-domain estimator," in *Proceedings of IMAC*, vol. 21. Society for Experimental Mechanics, 2003, pp. 183–192.

[3] M. El-Kafafy, "Design and validation of improved modal parameter estimators," Ph.D. dissertation, Vrije Universiteit Brussels Mechanical engineering dept, Brussels, Belgium: Faculty of Engineering, Department of Mechanical Engineering, 2013.

[4] P. Guillaume, P. Verboven, and S. Vanlanduit, "Frequency-domain maximum likelihood identification of modal parameters with confidence intervals," in *Proceedings of the international seminar on modal analysis*, vol. 1. Katholieke Universiteit Leuven, 1998.

[5] R. Allemang, D. Brown, and A. Phillips, "Survey of modal techniques applicable to autonomous/semi-autonomous parameter identification," pp. 3331–3372, 2010.

[6] B. Peeters, H. Van der Auweraer, P. Guillaume, and J. Leuridan, "The polymax frequency-domain method: a new standard for modal parameter estimation?" *Shock and Vibration*, vol. 11, no. 3, 4, pp. 395–409, 2004.

[7] A. W. Phillips, R. J. Allemang, and D. L. Brown, "Autonomous modal parameter estimation: methodology," in *Modal Analysis Topics, Volume 3*. Springer, 2011, pp. 363–384.

[8] J.-P. Dedieu and F. Tisseur, "Perturbation theory for homogeneous polynomial eigenvalue problems," *Linear algebra and its applications*, vol. 358, no. 1-3, pp. 71–94, 2003.

[9] W. Heylen, S. Lammens, and P. Sas, *Modal analysis theory and testing*. KUL. Faculty of engineering. Department of mechanical engineering. Division of production engineering, machine design and automation, 1997.

[10] N. Pandiya, C. Dindorf, and W. Desmet, "A single step modal parameter estimation algorithm - computing residues from numerator matrix coefficients of rational fractions," in *Proceedings of the 38th International Modal Analysis Conference, A Conference and Exposition on Structural Dynamics, Houston*. Springer International Publishing, 2020.

[11] N. Pandiya and W. Desmet, "Direct estimation of residues from rational-fraction polynomials as a single-step modal identification approach," *Journal of Sound and Vibration*, vol. 517, p. 116530, 2022.

[12] K. M. Vu, "An extension of the Faddeev's algorithms," in *2008 IEEE International Conference on Control Applications*, 9 2008.

[13] N. Pandiya *et al.*, "Improvements in modal parameter estimation under the derrp methodology," in *Proceedings of the 29th International Conference on Noise and Vibration engineering*. KU Leuven, 2020, pp. 2381–2394.

[14] N. Pandiya and W. Desmet, "Prediction of modal deflections and frequency response functions from experimental data: The longest vector approach," *Journal of Sound and Vibration*, vol. 530, p. 116964, 2022.

[15] H. Van der Auweraer and B. Peeters, "Discriminating physical poles from mathematical poles in high order systems: use and automation of the stabilization diagram," in *Proceedings of the 21st IEEE Instrumentation and Measurement Technology Conference (IEEE Cat. No.04CH37510)*, vol. 3, 2004, pp. 2193–2198.

[16] R. J. Allemang, "The modal assurance criterion–twenty years of use and abuse," *Sound and vibration*, vol. 37, no. 8, pp. 14–23, 2003.

[17] E. Reynders, J. Houbrechts, and G. De Roeck, "Fully automated (operational) modal analysis," *Mechanical systems and signal processing*, vol. 29, pp. 228–250, 2012.

[18] M. Scionti and J. Lanslots, "Stabilisation diagrams: Pole identification using fuzzy clustering techniques," *Advances in Engineering Software*, vol. 36, no. 11-12, pp. 768–779, 2005.

[19] M. Scionti, J. Lanslots, I. Goethals, A. Vecchio, H. Van der Auweraer, B. Peeters, and B. De Moor, "Tools to improve detection of structural changes from in-flight flutter data," in *Proceedings of the Eighth International Conference on Recent Advances in Structural Dynamics*, 2003.

[20] D. Lee, T.-S. Ahn, and H.-S. Kim, "A metric on the similarity between two frequency response functions," *Journal of Sound and Vibration*, vol. 436, pp. 32–45, 2018.

[21] M. El-Kafafy, B. Peeters, T. Geluk, and P. Guillaume, "The mlmm modal parameter estimation method: A new feature to maximize modal model robustness," *Mechanical Systems and Signal Processing*, vol. 120, pp. 465–485, 2019.